

Late Steps in the Formation of *E. coli* RNA Polymerase— λP_R Promoter Open Complexes: Characterization of Conformational Changes by Rapid [Perturbant] Upshift Experiments

Wayne S. Kontur¹, Ruth M. Saecker¹, Michael W. Capp¹
and M. Thomas Record Jr^{1,2*}

¹Department of Chemistry
University of Wisconsin-
Madison, 1101 University Ave.
Madison, WI 53706-1322, USA

²Department of Biochemistry
University of Wisconsin-
Madison, 433 Babcock Dr.
Madison, WI 53706-1544, USA

Received 4 August 2007;
received in revised form
24 October 2007;
accepted 20 November 2007
Available online
14 January 2008

The formation of the transcriptionally competent open complex (RP_o) by *Escherichia coli* RNA polymerase at the λP_R promoter involves at least three steps and two kinetically significant intermediates (I_1 and I_2). Understanding the sequence of conformational changes (rearrangements in the jaws of RNA polymerase, DNA opening) that occur in the conversion of I_1 to RP_o requires: (1) dissecting the rate constant k_d for the dissociation of RP_o into contributions from individual steps and (2) isolating and characterizing I_2 . To deconvolute k_d , we develop experiments involving rapid upshifts to elevated concentrations of RP_o -destabilizing solutes (“perturbants”: urea and KCl) to create a burst in the population of I_2 . At high concentrations of either perturbant, k_d approaches the same [perturbant]-independent value, interpreted as the elementary rate constant k_{-2} for $I_2 \rightarrow I_1$. The large effects of [urea] and [salt] on K_3 (the equilibrium constant for $I_2 \rightleftharpoons RP_o$) indicate that a large-scale folding transition in polymerase occurs and a new interface with the DNA forms late in the mechanism. We deduce that I_2 at the λP_R promoter is always unstable relative to RP_o , even at 0 °C, explaining previous difficulties in detecting it by using temperature downshifts. The division of the large positive enthalpy change between the late steps of the mechanism suggests that an additional unstable intermediate (I_3) may exist between I_2 and RP_o .

© 2007 Elsevier Ltd. All rights reserved.

Edited by P. J. Hagerman

Keywords: bacterial RNA polymerase; open complex formation; kinetics; solute effects; conformational changes

Introduction

To initiate RNA synthesis, RNA polymerase (RNAP) locally separates the complementary strands of promoter DNA around the transcription start site and

places the start site base on the template strand into its active site. Defining the cascade of conformational changes that occur during initiation and how they are regulated by promoter sequence and transcription factors is essential for understanding genetic expression, for defining the input into transcriptional networks, and for designing inhibitors of this essential process in disease-causing organisms. For the bacterial RNAP, open complex formation occurs in the absence of NTP hydrolysis or a helicase cofactor. For eukaryotic RNAP, additional protein cofactors are required to open the start site, although their roles in opening the DNA remain unclear.¹ Despite evolutionary differences in complexity, the extensive structural and functional homology between multi-

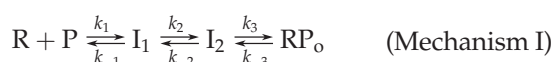
*Corresponding author. Department of Chemistry, University of Wisconsin-Madison, 1101 University Ave., Madison, WI 53706-1322, USA. E-mail address: mtrecord@wisc.edu.

Abbreviations used: RNAP, RNA polymerase; $S\kappa_{obs} = d\ln\kappa_{obs}/d\ln[\text{monovalent salt}]$, where κ_{obs} is a rate or equilibrium constant.

subunit RNAPs from all kingdoms² renders the relatively simple *Escherichia coli* enzyme a relevant model for the key steps in initiation, as well as providing a reference point for comparison with transcription by eukaryotic RNAP.

For *E. coli* RNAP holoenzyme (core enzyme (α_2 , β , β' , and ω subunits) and σ^{70} specificity subunit), formation of the transcriptionally competent open complex (RP_o) proceeds through a series of steps following the recognition of a specific promoter DNA sequence. In RP_o, the DNA is unpaired and unstacked from the AT-rich -10 hexamer to just downstream of the transcription start site, a span of ~14 base-pairs. At the λ P_R promoter, this open region extends from position -11 to +3,³⁻⁵ with numbering relative to the start site, +1. Despite decades of study of open complex formation, fundamental questions remain regarding this essential cellular process. For example, it is still unclear what conformational changes in RNAP are required for DNA opening and whether opening occurs in a single step or in several.

Addressing these mechanistic questions requires kinetic studies to provide essential information regarding the numbers of steps and intermediates involved in the overall process of forming RP_o and the characteristic rate and/or equilibrium constants of these steps. Kinetic data for formation and dissociation of RP_o involving *E. coli* RNAP (R) and the λ P_R promoter (P) is described by a mechanism consisting of a minimum of three steps with two kinetically significant intermediates:⁶⁻⁸



In Mechanism I, under conditions typically used in studies of open complex formation (4–42 °C, moderate salt concentration), I₁ rapidly equilibrates with free RNAP and promoter DNA on the time scale required for I₁ to convert to I₂, and I₂ rapidly equilibrates with RP_o on the time scale required for I₂ to convert to I₁. Notably, the interconversion I₁ ⇌ I₂ is the rate-limiting step in both the forward and reverse directions.^{6,9,10} Additional intermediates between the free species and I₁ and between I₂ and RP_o may exist. However, they are not included in Mechanism I because evidence for them has not been obtained from previous kinetic studies.

In excess RNAP, the kinetics of formation of open complexes between free RNAP and λ P_R promoter DNA are single exponential. In this case, measurements of the [RNAP]-dependence of the observed association rate constant are unambiguously interpreted in terms of K₁ (K₁ = k₁/k₋₁; the equilibrium constant for R + P ⇌ I₁) and k₂ (the rate constant for I₁ → I₂).^{9,10} The behaviors of K₁ and k₂ as functions of reaction conditions (such as temperature⁹ and solute concentrations¹¹) provide insight into the driving forces and molecular processes involved in the formation of I₁ from free RNAP and DNA and its

conversion to the subsequent transition state, (I₁–I₂)[‡]. For example, the small dependence of K₁ on urea concentration¹¹ implies that no large-scale folding transitions in RNAP occur concurrently with binding in R + P ⇌ I₁ (see Background).

Analogous information regarding the molecular processes that occur in the steps of the latter half of Mechanism I (the conversion of (I₁–I₂)[‡] into RP_o via I₂) is contained in the kinetics of conversion of RP_o back into free reactants (dissociation). At a minimum, the kinetically significant steps of irreversible dissociation (initiated by addition of an excess of the polyanionic competitor heparin, which acts as a DNA mimic to sequester free RNAP) are:¹⁰



(Mechanism II)

Previous studies of the kinetics of dissociation indicate that large-scale conformational changes occur in the latter half of Mechanism I. The large increases in the rate of dissociation with increasing concentrations of univalent salt^{7,12,13} and urea¹¹ indicate that a new RNAP-DNA interface forms and that ~120 amino acid residues fold in (I₁–I₂)[‡] ⇌ I₂ ⇌ RP_o (see Background). The large positive activation heat capacity change^{8,13} associated with the rate constant for dissociation (k_d; see Background) is also consistent with the hypothesis that a large-scale folding transition in RNAP occurs in (I₁–I₂)[‡] ⇌ I₂ ⇌ RP_o (as a heat capacity change in a biopolymer process often signals a protein folding event¹⁴). The strong acceleration of RP_o dissociation by the *in vivo* regulatory factors ppGpp and DksA at all promoters studied to date^{15,16} indicates that they bind to (I₁–I₂)[‡] and/or I₂ more strongly than to RP_o. These large effects are consistent with the existence of large-scale conformational changes occurring in the conversions between these species. For example, we have proposed that ppGpp and DksA accelerate dissociation by disfavoring the folding transition involved in converting I₂ to RP_o.¹¹

In I₁, promoter DNA around the transcription start site is unreactive to KMnO₄ and therefore presumably still double helical,^{3,17} while 14 base-pairs (-11 to +3) are deduced to be open in RP_o.³⁻⁵ Thus, DNA opening must occur in I₁ → I₂ and/or I₂ → RP_o. Large positive enthalpy changes are associated with these steps, consistent with the large enthalpic cost associated with melting DNA. A large positive activation energy (activation enthalpy) is observed for the conversion of I₁ to (I₁–I₂)[‡] (E_{a(2)} = 34 kcal/mol⁹), and the negative activation energy of dissociation indicates that the van't Hoff enthalpy change ΔH°₍₃₎ for I₂ ⇌ RP_o must be large and positive at low temperature.^{8,13}

Because RP_o and I₂ equilibrate rapidly on the time scale of converting I₂ to I₁, it has proven difficult to separate the steps that determine the dissociation kinetics (Mechanism II) and to isolate and char-

acterize I_2 . The goal of the present study is to unambiguously dissect, for the first time, the contributions of $RP_o \rightleftharpoons I_2$ and $I_2 \rightarrow I_1$ to the rate of open complex dissociation. This information can, in turn, be used to characterize the molecular processes occurring in the steps and to design experiments to trap and characterize the elusive I_2 .

One method of deconvoluting the kinetics of dissociation is a so-called "burst" experiment, in which a reaction variable is rapidly shifted in an attempt to destabilize RP_o and increase the population of I_2 . Use of temperature downshift bursts after initially forming RP_o at high temperatures were attempted based on the conclusion that $\Delta H^\circ_{(3)}$ for $I_2 \rightleftharpoons RP_o$ is large and positive and the inference that a downshift in temperature will therefore rapidly depopulate RP_o .^{3,18–20} However, the difficulty of performing a temperature downshift rapidly, the temperature dependence of the rate of $KMnO_4$ reactivity (activation energy ~ 8 kcal/mol; M. W. C., unpublished data), and the possibility of artifacts (such as off-pathway complexes formed in the downshifts^{21,22}) may have complicated the interpretations of these experiments.

Here we have designed isothermal burst (upshift) experiments, in which pre-formed open complexes are rapidly shifted to elevated concentrations of either urea or KCl and the dissociation kinetics are followed. We find that the rate constant for dissociation of open complexes (k_d) reaches or approaches a [urea] and [KCl]-independent value at both 10 and 37 °C, signifying that either k_{-3} ($RP_o \rightarrow I_2$) or k_{-2} ($I_2 \rightarrow I_1$) is independent of [perturbant]. Based on an analogy between our data and the effect of [urea] on the kinetics and equilibria of protein folding, we propose that the plateau value of k_d represents the rate constant k_{-2} , and that the entire effect of [urea] and of [salt] on k_d are contained in $RP_o \rightleftharpoons I_2$ (i.e. k_{-3} and k_3). Implications of these results for the nature of I_2 and of the steps converting I_1 to RP_o are discussed.

Background

Formulation of the dissociation rate constant k_d

For systems where the kinetics of dissociation of open complexes are single exponential (as observed for the λP_R promoter under almost all conditions studied^{6,7,11}), the dissociation rate constant k_d is interpreted without approximation as:¹⁰

$$k_d = \frac{k_{-2}k_{-3}}{k_{-2} + k_{-3} + k_3} = \frac{k_{-2}}{1 + K_3 + k_{-2}/k_{-3}} \quad (1)$$

where $K_3 = k_3/k_{-3}$.

Under conditions where the interconversion of RP_o and I_2 in Mechanism II rapidly equilibrates on the time scale required for I_2 to convert to I_1 ($k_3 \gg k_{-2}$), deduced experimentally from the negative

activation energy of k_d ,^{6,8,13} equation (1) can be simplified, depending on the relative magnitude of K_3 :¹⁰

$$k_d = \frac{k_{-2}}{1 + K_3} \quad \text{where } K_3 \sim 1 \quad (2a)$$

or

$$k_d = \frac{k_{-2}}{K_3} \quad \text{where } K_3 \gg 1 \quad (2b)$$

Interpretation of the effect of non-denaturing concentrations of urea on a biopolymer process and application to the study of the kinetics of open complex formation

Urea has been shown to interact preferentially (i.e. relative to interactions with water) primarily with amide groups (specifically with the polar N and O atoms) of proteins and model compounds.^{23–30} Preferential interactions of urea with other groups on proteins and nucleic acids (such as predominantly non-polar or charged groups) have not been detected in studies with biopolymers.^{24,25} We have quantified this interaction per unit of polar amide surface area ($ASA_{\text{polar amide}}$; \AA^2),^{24,28,30} thus making [urea] an effective quantitative probe of changes in the solvent exposure of amide surface area associated with biopolymer processes:

$$d \ln K_{\text{obs}} / d m_{\text{urea}} = (1.4 \times 10^{-3}) \Delta ASA_{\text{polar amide}} \quad (3)$$

where K_{obs} is the observed equilibrium quotient for a biopolymer process and $\Delta ASA_{\text{polar amide}}$ is the change in the amount of water-accessible polar amide surface area in converting the reactant state to the product state. A test of the usefulness of [urea] as a probe of $\Delta ASA_{\text{polar amide}}$ was provided by a study of lac repressor binding to operator DNA; the observed effect of [urea] on the binding constant K_{obs} agrees with that predicted from structural information on the amount of polar amide surface buried in complex formation.³⁰

This method of analysis has been used to interpret the [urea]-dependences of K_1 , k_2 , and k_d in Mechanisms I and II.¹¹ The moderate initial dependence of K_1 on [urea] is consistent with the polar amide surface area known or predicted to be buried in the large RNAP-DNA interface formed in $R+P \rightleftharpoons I_1$, without having to invoke additional large-scale folding transitions. The lack of a dependence of k_2 on [urea] implies that there is no net exposure of polar amide surface in the conversion of I_1 to the subsequent transition state (I_1-I_2)[‡]. The large dependence of k_d on [urea] was interpreted as a large-scale folding transition in a region of RNAP in (I_1-I_2)[‡] $\rightleftharpoons RP_o$. Specifically, we proposed that disordered regions in the C terminus of the β' subunit, including the downstream jaw, fold in $I_2 \rightleftharpoons RP_o$.

Experiments performed at moderate urea concentrations under reversible conditions, where the kinetics of the association and dissociation reactions can be measured simultaneously (Supporting Infor-

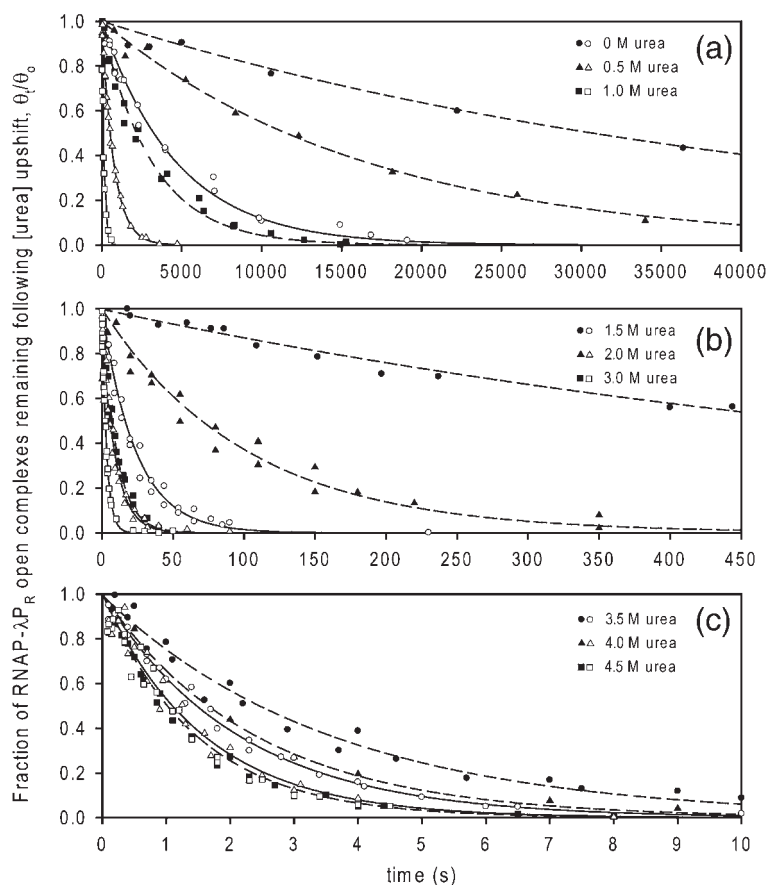


Figure 1. Dissociation of RNA polymerase (RNAP)- λP_R promoter open complexes after upshifts in urea concentration. Pre-formed open complexes in dissociation buffer (DB) were mixed with a solution of DB containing urea and heparin to obtain the urea concentrations listed. Data are plotted as the fraction of DNA originally bound in open complexes remaining bound after upshift (θ_t/θ_0). Filled symbols represent data taken at 37 °C. Open symbols represent data taken at 10 °C. Lines are fits of the data to a single exponential decay (equation (4)). Broken lines are fits to the 37 °C data, and continuous lines are fits to the 10 °C data. Rate constants (k_d) from the fits are contained in Table 1. (a) Upshifts to 0 (circles), 0.5 (triangles), and 1.0 (squares) M urea. (b) Upshifts to 1.5 (circles), 2.0 (triangles), and 3.0 (squares) M urea. (c) Upshifts to 3.5 (circles), 4.0 (triangles), and 4.5 (squares) M urea.

mation of¹¹ and unpublished data), result in values for k_d that are the same within error as those obtained from irreversible dissociation experiments at the same urea concentrations. This result provides evidence that the intermediates involved in the forward and reverse processes in the presence of perturbant are the same.

Results

The dissociation of RNAP-promoter open complexes following upshifts in perturbant (urea or KCl) concentration shows single exponential kinetics

The rate of dissociation of open complexes (RP_o) formed between *E. coli* RNAP and λP_R promoter DNA is greatly accelerated by increasing concentrations of urea¹¹ and salt.^{6,7,12} We monitored the dissociation of pre-formed open complexes following a rapid upshift in either [urea] (up to 5.0 M) or [KCl] (up to 1.10 M) in order to dissect the contributions of $RP_o \rightleftharpoons I_2$ and $I_2 \rightarrow I_1$ (Mechanism II) to the overall [perturbant]-dependences of k_d . (Evidence that these experiments monitor the dissociation kinetics of RP_o by Mechanism II and not by an alternative mechanism induced by high [salt] or [urea] (such as holoenzyme or DNA denaturation) is presented in Analysis.) Representative data for these

dissociation experiments are shown in Figures 1 ([urea] upshifts) and 2 ([KCl] upshifts). These data are well fit by single-exponential decays (equation (4), Methods) under every set of reaction conditions studied; fits are represented by continuous lines for the 10 °C data and broken lines for the 37 °C data. Values of the dissociation rate constant k_d from fits to equation (4) are given in Tables 1 (for the [urea] upshifts) and 2 (for the [KCl] upshifts). The single exponential character of the data validates the use of

Table 1. Values of the rate constant for the dissociation of open complexes (k_d) following upshift in urea concentration

[urea] (M)	k_d (s^{-1}) ^a	
	37 °C	10 °C
0	$1.9(\pm 0.6) \times 10^{-5}$	$2.1(\pm 0.2) \times 10^{-4}$
0.5	$6.0(\pm 1.2) \times 10^{-5}$	$1.35(\pm 0.06) \times 10^{-3}$
1.0	$3.2(\pm 0.6) \times 10^{-4}$	$7.1(\pm 0.5) \times 10^{-3}$
1.5	$1.4(\pm 0.3) \times 10^{-3}$	$4.1(\pm 0.7) \times 10^{-2}$
2.0	$8.9(\pm 2.2) \times 10^{-3}$	$1.2(\pm 0.2) \times 10^{-1}$
2.5	$3.8(\pm 1.5) \times 10^{-2}$	$2.0(\pm 0.2) \times 10^{-1}$
3.0	$9.4(\pm 1.4) \times 10^{-2}$	$3.1(\pm 0.2) \times 10^{-1}$
3.5	$2.5(\pm 0.7) \times 10^{-1}$	$4.7(\pm 0.2) \times 10^{-1}$
4.0	$5.5(\pm 2.2) \times 10^{-1}$	$7.0(\pm 1.2) \times 10^{-1}$
4.5	$6.9(\pm 0.4) \times 10^{-1}$	$7.0(\pm 0.6) \times 10^{-1}$
5.0	1.4 ± 0.2	–

^a k_d is calculated by fitting the dissociation data represented in Figure 1 with equation (4).

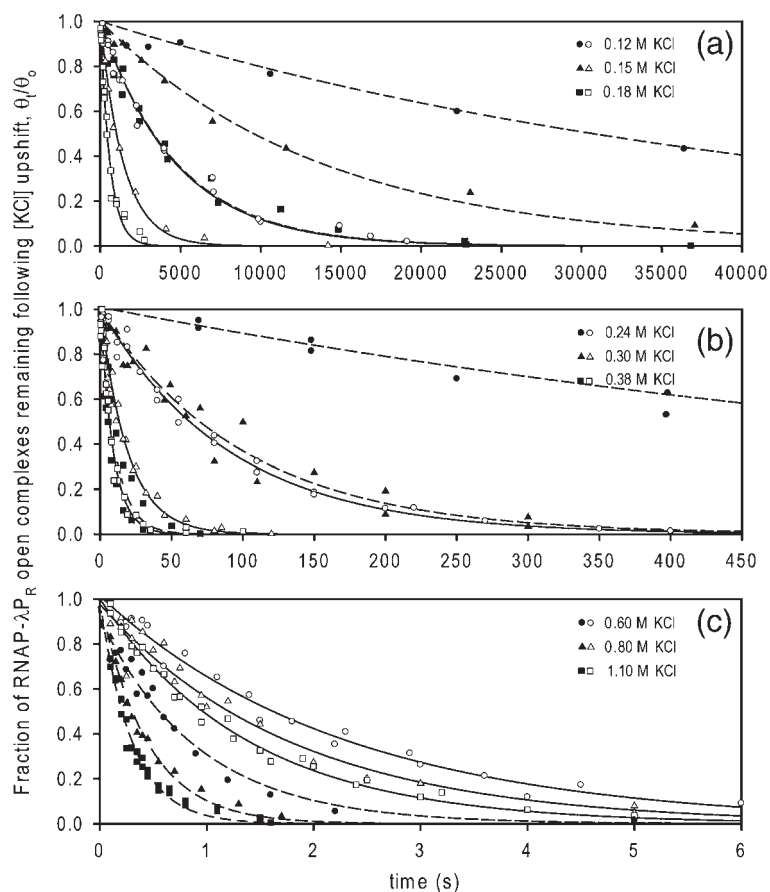


Figure 2. Dissociation of RNAP- λP_R promoter open complexes after upshifts in KCl concentration. Pre-formed open complexes in dissociation buffer (DB) were mixed with a solution of DB containing additional KCl and heparin to obtain the KCl concentrations listed. Data are plotted as the fraction of DNA originally bound in open complexes remaining bound after upshift (θ_t/θ_0). Filled symbols represent data taken at 37 °C. Open symbols represent data taken at 10 °C. Lines are fits of the data to a single exponential decay (equation (4)). Broken lines are fits to the 37 °C data, and continuous lines are fits to the 10 °C data. Rate constants (k_d) from the fits are contained in Table 2. (a) Upshifts to 0.12 (circles), 0.15 (triangles), and 0.18 (squares) M KCl. (b) Upshifts to 0.24 (circles), 0.30 (triangles), and 0.38 (squares) M KCl. (c) Upshifts to 0.60 (circles), 0.80 (triangles), and 1.10 (squares) M KCl. Note: The data at 0 M urea in Figure 1 are the same as the data at 0.12 M KCl in Figure 2 (re-plotted for comparison).

equation (1) (see Background) in the analysis of all values of k_d .¹⁰

The rate of open complex dissociation is strongly driven by [perturbant] at low perturbant concentrations but independent of [perturbant] at high perturbant concentrations

In Figure 3, the natural logarithm of k_d ($\ln k_d$) is plotted *versus* [urea] (a) or \ln [KCl] (b). At the lowest concentrations of both urea (up to ~ 1.5 M at 10 °C and ~ 2.5 M at 37 °C) and KCl (up to ~ 0.30 M at 10 °C and ~ 0.48 M at 37 °C), $\ln k_d$ increases dramatically with increasing [perturbant] (linearly *versus* [urea] and with a slight positive (upward) curvature *versus* \ln [KCl]). At higher concentrations of both perturbants, the rate of open complex dissociation becomes less dependent on [perturbant], resulting in negative (downward) curvature in the data in Figure 3. For example, while $d\ln k_d/d[\text{urea}]$ at 10 °C between 0 M urea and 0.5 M urea is $\sim 3.5 \text{ M}^{-1}$, $d\ln k_d/d[\text{urea}]$ is only $\sim 1 \text{ M}^{-1}$ between 2.0 M urea and 3.0 M urea (Figure 3(a)). Likewise, at 37 °C, between 0.30 M KCl and 0.38 M KCl, $d\ln k_d/d\ln[\text{KCl}] = \sim 9.3$, while between 0.48 M KCl and 0.60 M KCl, $d\ln k_d/d\ln[\text{KCl}] = \sim 5.4$ (Figure 3(b)).

At the highest concentrations of either perturbant, the rate of open complex dissociation becomes essentially independent of [perturbant]. This is particularly evident in Figure 3(b), where k_d appears to have reached a [KCl]-independent plateau at both

10 and 37 °C (for example, at 37 °C, $k_d = 2.3(\pm 0.8) \text{ s}^{-1}$ at 0.80 M KCl and $3.3(\pm 0.2) \text{ s}^{-1}$ at 1.10 M KCl (Figure 2(c) and Table 2)). Similarly, in Figure 3(a), k_d at 10 °C appears to have reached a [urea]-independent plateau ($k_d = 7.0(\pm 1.2) \times 10^{-1} \text{ s}^{-1}$ at 4.0 M urea and $7.0(\pm 0.6) \times 10^{-1} \text{ s}^{-1}$ at 4.5 M urea (Figure 1(c) and Table 1)). While k_d at 37 °C is still increasing with [urea] at the highest urea concentration studied ($k_d = 6.9(\pm 0.4) \times 10^{-1} \text{ s}^{-1}$ at 4.5 M urea and $1.4(\pm 0.2) \text{ s}^{-1}$ at 5.0 M urea (Figure 1(c) and Table 1)), it also appears to be gradually approaching a plateau at even higher [urea] (Figure 3(a)).

Table 2. Values of the rate constant for the dissociation of open complexes (k_d) following upshift in KCl concentration

[KCl] (M)	k_d (s^{-1}) ^a	
	37 °C	10 °C
0.12	$1.9(\pm 0.6) \times 10^{-5}$	$2.1(\pm 0.2) \times 10^{-4}$
0.15	$7.3(\pm 0.7) \times 10^{-5}$	$6.9(\pm 0.4) \times 10^{-4}$
0.18	$1.9(\pm 0.4) \times 10^{-4}$	$1.6(\pm 0.2) \times 10^{-3}$
0.24	$1.3(\pm 0.1) \times 10^{-3}$	$1.15(\pm 0.07) \times 10^{-2}$
0.30	$1.0(\pm 0.3) \times 10^{-2}$	$5.3(\pm 0.9) \times 10^{-2}$
0.38	$9.1(\pm 5.2) \times 10^{-2}$	$1.1(\pm 0.1) \times 10^{-1}$
0.48	$4.8(\pm 0.6) \times 10^{-1}$	—
0.60	1.6 ± 0.7	$4.2(\pm 0.7) \times 10^{-1}$
0.80	2.3 ± 0.8	$5.5(\pm 1.4) \times 10^{-1}$
1.10	3.3 ± 0.2	$7.3(\pm 0.6) \times 10^{-1}$

^a k_d is calculated by fitting the dissociation data (see for example Figure 2) with equation (4).

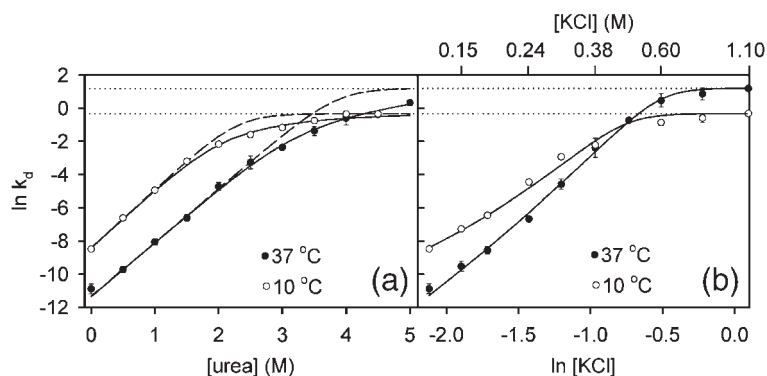


Figure 3. The natural logarithm (\ln) of the dissociation rate constant k_d (from fits of the kinetic data represented in Figures 1 and 2 to equation (4)) plotted versus [urea] (a) and \ln [KCl] (b). Filled points are for data taken at 37 °C; open points are for data taken at 10 °C. In (a), continuous lines are fits of the data to an expression (utilizing equations (5), (7), and (8)) in which dependences of the equilibrium constant K_3 ($I_2 \rightleftharpoons RP_o$) and the rate constant k_{-3} ($RP_o \rightarrow I_2$) on [urea] are incorporated into the general expression for k_d (equation (1)). Broken lines are fits of the data to an expression (utilizing equations (6) and (7)) in which only the dependence of K_3 on [urea] is incorporated into a simplified expression for k_d (equation (2a)). In (b), continuous lines are fits of the data to an expression (utilizing equations (6), (9)–(11)) in which a dependence of K_3 on [KCl] was incorporated into the simplified expression for k_d (equation (2a)). Horizontal dotted lines represent values of $\ln k_{-2}$ determined from the fits.

The dissociation of open complexes is characterized by a negative activation energy at low perturbant concentrations and a positive activation energy at high perturbant concentrations

At the lowest urea and KCl concentrations studied, k_d is much larger at 10 °C than at 37 °C (Figure 3; Tables 1 and 2). This difference is vividly demonstrated in Figures 1(a) and 2(a): dissociation of open complexes is much faster at 10 °C than at 37 °C in 0, 0.5, and 1.0 M urea (Figure 1(a)) and in 0.12, 0.15, and 0.18 M KCl (Figure 2(a)). The negative activation energy for k_d implies that a rapidly equilibrating initial step (or steps) precedes the rate-determining step in dissociation (because an elementary rate constant cannot have a negative activation energy). The earlier observation of this negative activation energy originally motivated the inclusion of a second kinetically significant intermediate (I_2) into Mechanism I.^{6,8,19}

As the perturbant concentrations are increased, the differences between k_d at 10 °C and 37 °C decrease (i.e. the negative activation energy in each perturbant decreases in magnitude) until, after upshift to some [urea] and [KCl], the values of k_d at 10 °C and 37 °C converge (where the activation energy is zero) (Figure 3; Tables 1 and 2). As seen in Figure 1(c), this occurs at ~ 4.5 M urea, where open complexes dissociate at roughly the same rate at 10 °C and 37 °C (k_d is $6.9(\pm 0.4) \times 10^{-1} \text{ s}^{-1}$ at 37 °C and $7.0(\pm 0.6) \times 10^{-1} \text{ s}^{-1}$ at 10 °C). In Figure 2(b), the rate of dissociation is essentially independent of temperature at 0.38 M KCl ($k_d = 9.1 (\pm 5.2) \times 10^{-2} \text{ s}^{-1}$ at 37 °C and $1.1(\pm 0.1) \times 10^{-1} \text{ s}^{-1}$ at 10 °C).

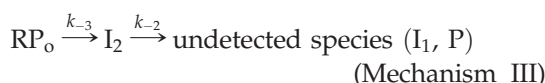
At concentrations of KCl higher than 0.38 M, k_d is significantly larger at 37 °C than at 10 °C (Figure 3(b) and Table 2); this is dramatically apparent in Figure 2(c), where dissociation of open complexes is clearly faster at 37 °C than at 10 °C in 0.60, 0.80, and 1.10 M KCl. This temperature dependence of dissociation at high [KCl] results in a positive activation energy for the process. The data indicate that a positive activation energy is likely at high concentrations of

urea as well. While k_d is the same at 10 °C and 37 °C at 4.5 M urea (the highest concentration for which there is data at both temperatures), k_d has reached its [urea]-independent value already by 4.5 M urea at 10 °C (Figure 3(a) and Table 1), and so would be expected to have that same value at all higher concentrations of urea. However, at 37 °C, k_d is still increasing: at 5.0 M urea, $k_d = 1.4(\pm 0.2) \text{ s}^{-1}$. Thus, at urea concentrations greater than 4.5 M, k_d is likely larger at 37 °C than at 10 °C. Because values of k_d at high [KCl] and [urea] at both 10 °C and 37 °C are independent of perturbant concentration, the positive activation energy of k_d in this regime is also independent of perturbant concentration.

Analysis

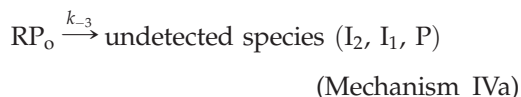
Interpretation of k_d at high perturbant concentrations: the rate of dissociation is determined by the rate of $I_2 \rightarrow I_1$

The simplest interpretation of the [perturbant]-independent positive activation energy for open complex dissociation at high perturbant concentrations (represented by the higher plateau value of k_d at 37 °C than at 10 °C in Figure 3) is that I_2 no longer rapidly converts back to the higher enthalpy state RP_o on the time scale over which I_2 converts to I_1 . In order for the rapid equilibrium in $I_2 \rightleftharpoons RP_o$ to break down, $I_2 \rightarrow I_1$ must become faster than $I_2 \rightarrow RP_o$, resulting in a mechanism of dissociation consisting of two sequential uni-directional steps at high [perturbant]:

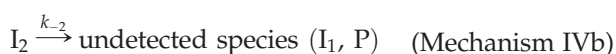


In general, analysis of Mechanism III for the situation where both RP_o and I_2 are detectable and where k_{-3} and k_{-2} are of comparable magnitude yields a lag phase in the dissociation of detectable complexes. Since the data in Figures 1(c) and 2(c)

(for dissociation of detectable complexes at high perturbant concentrations) are well fit by a single exponential decay (without an apparent lag phase), one of the rate constants in the back direction, either k_{-2} or k_{-3} , must be large enough that it does not contribute to the overall observable kinetics of dissociation. In this high [perturbant] regime, dissociation of detectable complexes must therefore be represented by one or the other of the following mechanisms:



or



For Mechanism IVa to be applicable, k_{-2} would have to exceed k_{-3} by enough so that no I_2 accumulates on the time scale of the conversion of RP_o to I_2 . For Mechanism IVb to be applicable, k_{-3} would have to exceed k_{-2} by enough so that all RP_o converts to I_2 before significant dissociation of I_2 commences (and within the time resolution of the experiment). Because the plateaus at high perturbant concentrations are independent of [perturbant], whichever rate constant determines k_d in this regime (either k_{-3} or k_{-2}) is independent of [perturbant].

Although the data alone do not allow us to distinguish between Mechanisms IVa and IVb because of the symmetry between k_{-2} and k_{-3} in the general expression for k_d (equation (1)), we propose that Mechanism IVb describes the dissociation of detectable complexes at high [perturbant]. Our reasoning is based on an analogy between the [urea]-dependent step in open complex formation and the two-state process of folding a single-domain globular protein. In general, for proteins for which the rates of folding (k_{fold}) and unfolding (k_{unfold}) have been determined as functions of urea concentration, the overall [urea]-dependence of the equilibrium constant ($K_{\text{obs}} = k_{\text{fold}}/k_{\text{unfold}}$) is distributed to some extent (between 30% and 70% of the overall effect on each) between k_{fold} and k_{unfold} .³¹ The rate constants k_2 ($\text{I}_1 \rightarrow \text{I}_2$) and k_{-2} ($\text{I}_2 \rightarrow \text{I}_1$) are the forward and reverse elementary rate constants that make up the equilibrium K_2 ($\text{I}_1 \rightleftharpoons \text{I}_2$); because we previously found that k_2 is independent of [urea],¹¹ it is unlikely that k_{-2} would contain a significant [urea]-dependence. Thus, it is most likely that the [urea]-dependence is contained within k_3 and k_{-3} . (While a situation in which the [urea]-dependence of a biopolymer process is fully contained within only one of the rate constants that make up the equilibrium constant for the process may not be physically impossible, to our knowledge no examples of it exist.)

The behavior of k_d at high concentrations of urea and KCl strongly supports our conclusion that Mechanism II (at low [perturbant]) and Mechanism IVb (at high [perturbant]) characterize the dissociation of RNAP-promoter complexes, and that other

mechanisms (such as RNAP or DNA denaturation) are not significant. In particular, if perturbant-induced denaturation were occurring, we would expect the rate of dissociation to continue increasing with perturbant concentration, rather than reaching [perturbant]-independent plateaus, as are seen in the data. Moreover, the native forms of RNAP holoenzyme³² and DNA³³ are stable at high salt concentrations, so upshifts in KCl concentration cannot be inducing denaturation. The observation that the rate of dissociation at high [perturbant] is independent of the identity of perturbant (most explicitly evident at 10 °C; Figure 3) implies that the same dissociation process is occurring at both high [urea] and high [KCl]. Thus, we conclude that if other salt or urea-induced processes do occur, they do so only after the transition state ($\text{I}_1\text{-I}_2$)[‡] has been formed in the dissociation direction, and therefore do not influence the observed kinetics of dissociation.

The step $\text{I}_1 \rightleftharpoons \text{I}_2$ is highly endothermic

From the values of k_{-2} at 10 °C and 37 °C (Table 3), we estimate the activation energy for k_{-2} ($E_{a(-2)} = -R\Delta \ln k_{-2} / \Delta(1/T)$) to be 9.9 kcal/mol. This activation energy is smaller than that of k_2 ($E_{a(2)} = 34$ kcal/mol),⁹ resulting in an estimated enthalpy change for the overall step ($\text{I}_1 \rightleftharpoons \text{I}_2$) that is large and positive ($\Delta H_2^\circ = 24$ kcal/mol). Our calculation assumes that there is no activation heat capacity change for k_{-2} ($\Delta C_{p(-2)}^\ddagger = \Delta E_{a(-2)} / \Delta T \sim 0$), and thus that $E_{a(-2)}$ is constant between 10 °C and 37 °C. This assumption is consistent with the observed lack of an activation heat capacity change for the forward rate constant k_2 ,⁹ and is analogous to the argument (above) that the lack of a [urea]-dependence of k_2 implies that k_{-2} is independent of [urea] as well. A heat capacity change in a biopolymer process, like a [urea]-dependence, is often a sign of a conformational change in which biopolymer surface is either buried from or exposed to the solvent.¹⁴ We propose that the [urea]-dependence and the heat capacity change in k_d both result from the same folding transition in

Table 3. Parameters from the analysis of the [urea] and [KCl] upshifts at 37 °C and 10 °C

	37 °C	10 °C
k_{-2} (s ⁻¹)	3.3±0.7	7.2(±0.7)×10 ⁻¹
K_3^{a}	2.7(±0.9)×10 ⁵	3.2(±0.6)×10 ³
$\text{dln}K_3/\text{d[urea]}^{\text{b}}$	-3.3±0.2 M ⁻¹	-3.5±0.1 M ⁻¹
k_{-3}^{c} (s ⁻¹) ^{a,c}	1.1(±0.7)×10 ⁻²	3.3(±1.0)×10 ⁻²
k_3^{c} (s ⁻¹) ^{a,d}	3.0(±2.2)×10 ³	1.0(±0.4)×10 ²
$\text{dln}k_{-3}/\text{d[urea]}^{\text{c}}$		1.1±0.2 M ⁻¹
$\text{dln}k_3/\text{d[urea]}^{\text{e}}$	-2.2±0.2 M ⁻¹	-2.5±0.2 M ⁻¹

^a X^o is the value of X in DB (containing 0.12 M KCl and no urea).

^b Determined from a fit of the linear regions of the data in Figure 3(a) (0–1.5 M urea at 10 °C and 0–2.5 M urea at 37 °C).

^c Calculated from fits of the data in Figure 3(a) to equation (5). Value constrained to be temperature-independent; see Methods.

^d Calculated from values of K_3 ($=k_3/k_{-3}$) and k_{-3} in this Table.

^e Calculated from: $\text{dln}k_3/\text{d[urea]} = \text{dln}K_3/\text{d[urea]} + \text{dln}k_{-3}/\text{d[urea]}$.

RNAP; the extension of this proposal is that both are contained in the same step ($I_2 \rightleftharpoons RP_o$).

Interpretation of k_d at low perturbant concentrations: the [perturbant]-dependence of the rate of dissociation is determined by the [perturbant]-dependence of $RP_o \rightleftharpoons I_2$

As seen in Figure 3, k_d increases dramatically with increasing [perturbant] at low perturbant concentrations. The logarithm of k_d increases linearly with increasing [urea] (up to ~ 1.5 M urea at 10 °C and ~ 2.5 M urea at 37 °C; Figure 3(a)) and non-linearly (with slight upward curvature) with \ln [KCl] (up to ~ 0.30 M KCl at 10 °C and to ~ 0.48 M KCl at 37 °C; Figure 3(b)). These trends in k_d correspond closely to the behaviors expected for the equilibrium constants for protein unfolding and for disruption of a protein-DNA interface, respectively. In studies of protein unfolding, $\ln K_{obs}$ is almost invariably a linear function of [urea] (giving rise to the so-called “ m -value”), even to zero urea.²⁹ For studies of the dissociation of positively charged ligands from DNA in the presence of both univalent salt and Mg^{2+} , $\ln K_{obs}$ shows a non-linear dependence on \ln [univalent salt], with curvature resulting from the [univalent salt]-dependent association of Mg^{2+} with the DNA phosphate backbone.³⁴ The trends in the data at low [perturbant] in Figure 3, coupled with the assumption that k_{-2} is independent of [perturbant], imply that the denominator of the expression for k_d (equation (1)) is completely dominated by K_3 ($K_3 \gg 1 + k_{-2}/k_{-3}$). The expression for k_d at low [perturbant] can therefore be simplified to equation (2b): $k_d = k_{-2}/K_3$. Thus, the initial dependences of k_d on [urea] and [KCl] are equal in magnitude to the dependences of K_3 on those perturbants: $d \ln k_d / d[\text{urea}] = -d \ln K_3 / d[\text{urea}]$ and $S k_d (= d \ln k_d / d \ln [\text{KCl}]) = -S K_3$.

Fits of the linear regions of the [urea] upshift data in Figure 3(a) give the following values of $d \ln K_3 / d[\text{urea}]$: $-3.3(\pm 0.2) \text{ M}^{-1}$ at 37 °C and $-3.5(\pm 0.1) \text{ M}^{-1}$ at 10 °C. These dependences agree well with that determined previously at 17 °C over a smaller range of urea concentrations ($d \ln k_d / d[\text{urea}] (= -d \ln K_3 / d[\text{urea}]) = 3.1(\pm 0.1) \text{ M}^{-1}$ from 0 to 0.6 M urea¹¹). Using equation (3) (see Background), these values of $d \ln K_3 / d[\text{urea}]$ reveal that $\sim 2.4 \times 10^3 \text{ \AA}^2$ of polar amide biopolymer surface (corresponding to ~ 120 amino acid residues) is buried in the conversion of I_2 to RP_o .

I_2 is unstable under typical transcription assay conditions

One implication of the values of k_{-2} and K_3 obtained from the fits of the upshift data (Table 3) is that I_2 is unstable relative to both I_1 and RP_o at the λ_{PR} promoter under typical assay conditions. In dissociation buffer, the equilibrium constant K_2 for $I_1 \rightleftharpoons I_2$ is $\sim 3 \times 10^{-3}$ at 10 °C and ~ 0.2 at 37 °C (with $K_2 = k_2/k_{-2}$ calculated using the values of k_{-2} from Table 3 and values of k_2 determined previously⁹). The equilibrium constant K_3 for $I_2 \rightleftharpoons RP_o$ is $3.2(\pm 0.6) \times 10^3$

at 10 °C and $2.7 (\pm 0.9) \times 10^5$ at 37 °C (Table 3). Calculation of K_2 and K_3 between 0 and 42 °C (data not shown) shows that essentially none of the promoter DNA exists as I_2 at equilibrium at any temperature, explaining previous difficulties in isolating and characterizing it. Notably, at 0 °C, K_3 is calculated to be ~ 120 , indicating that our previous attempt to rapidly populate I_2 through means of a temperature downshift to 0 °C³⁵ was unsuccessful and therefore incorrectly interpreted.

Interpretation of k_d at intermediate perturbant concentrations

At moderate perturbant concentrations, K_3 has decreased by enough such that it contributes less to the denominator of k_d than it did at low concentrations (where it so completely dominated the denominator that $d \ln k_d / d(\ln)[\text{perturbant}] = -d \ln K_3 / d(\ln)[\text{perturbant}]$), but not by so much that it is negligible compared to unity (as is the case at high [perturbant], where $k_d = k_{-2}$). Thus, the dependences of K_3 on [perturbant] contribute progressively less to the overall dependences of k_d , and these overall dependences begin to decrease in magnitude. These transition regions between the low ($k_d = k_{-2}/K_3$) and high ($k_d = k_{-2}$) [perturbant] regimes are characterized by downward (negative) curvature in the trends in $\ln k_d$ with [urea] (~ 1.5 – 3.5 M at 10 °C and > 2.5 M at 37 °C) and with \ln [KCl] (~ 0.30 – 0.80 M at 10 °C and ~ 0.48 – 0.80 M at 37 °C) (Figure 3).

The exact dependences of k_d on [perturbant] in the transition regions depend on the relationship between the individual rate constants that comprise k_d : k_{-2} , k_3 , and k_{-3} . There are two possible scenarios: either all three terms ($1 + K_3 + k_{-2}/k_{-3}$) contribute to the denominator of k_d (equation (1)), or only two terms ($1 + K_3$) contribute to the denominator of k_d (equation (2a)). These scenarios are considered below for the [urea] and [KCl] upshifts.

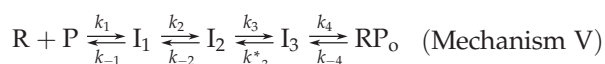
Intermediate urea concentrations: evidence that an additional kinetically significant intermediate (I_3) may exist between I_2 and RP_o

We initially attempted fits of $\ln k_d$ versus [urea] (Figure 3(a)) to equation (6) (Methods), in which we assume that only the expression $1 + K_3$ (and not k_{-2}/k_{-3}) contributes to the denominator of k_d throughout the entire range of urea concentrations studied (using values of k_{-2} , K_3 , and $d \ln K_3 / d[\text{urea}]$ in Table 3 for the fits). It is visually apparent that these fits, shown as broken lines in Figure 3(a), are not optimal. While the fits are good at low and high [urea], the fitted curves lie systematically and significantly above the data points at intermediate [urea] (i.e. k_d approaches the plateau values of k_{-2} at high [urea] more slowly than predicted by the fits). While this discrepancy exists for both the 10 °C and 37 °C data sets, it is much more pronounced at 37 °C.

One possible reason for this discrepancy is that the k_{-2}/k_{-3} term contributes significantly to k_d in this range of urea concentrations. To test this possibility,

the data in Figure 3(a) were refit to equation (5) (Methods), in which the k_{-2}/k_{-3} term is included. The fits to equation (5), shown as continuous lines, clearly agree with the experimental data at intermediate urea concentrations better than the fits to equation (6). Values of k_{-3}^o (the value in dissociation buffer in the absence of urea) and $\text{dln}k_{-3}/\text{d[urea]}$ for 10 °C and 37 °C determined from these fits are given in Table 3.

One interesting feature of these fits is that the resultant value of k_{-3}^o at 10 °C ($3.3 (\pm 1.0) \times 10^{-2} \text{ s}^{-1}$) is larger than the value at 37 °C ($1.1 (\pm 0.7) \times 10^{-2} \text{ s}^{-1}$). This difference results from the fact that the discrepancy between the data and the fit to equation (6) for the 37 °C data set is larger than that for the 10 °C data set; thus, the 37 °C data set requires a larger value of k_{-2}/k_{-3} in the denominator of the expression for k_d to correct for the discrepancy. The resulting negative activation energy for k_{-3} ($E_{a(-3)} \sim -7 \text{ kcal/mol}$, based on a two-point fit) implies that, in the context of this analysis, k_{-3} is not an elementary rate constant. If k_{-3} were in fact non-elementary, it would contain one or more additional equilibrium steps, resulting in the following minimal mechanism:



where $k_3 \gg k_{-2}$ (rapid equilibrium in $\text{I}_2 \rightleftharpoons \text{I}_3$) and $k_4 \gg k_{-3}^*$ (rapid equilibrium in $\text{I}_3 \rightleftharpoons \text{RP}_o$). The quantity k_{-3} from Mechanism I ($\text{RP}_o \rightarrow \text{I}_2$) would be a composite rate constant containing k_{-3}^* , k_4 , and k_{-4} .

From the fits of the data to equation (5), the [urea]-dependence of $\text{I}_2 \rightarrow \text{RP}_o$ ($\text{dln}k_3/\text{d[urea]} = -2.2 (\pm 0.2) \text{ M}^{-1}$ at 37 °C) is larger in magnitude than that of the reverse process $\text{RP}_o \rightarrow \text{I}_2$ ($\text{dln}k_{-3}/\text{d[urea]} = 1.1 (\pm 0.2) \text{ M}^{-1}$). While the [urea]-dependence of $\text{RP}_o \rightarrow \text{I}_2$ (k_{-3}) could conceivably be distributed between $\text{I}_3 \rightarrow \text{I}_2$ (k_{-3}^*) and $\text{I}_3 \rightleftharpoons \text{RP}_o$ ($K_4 = k_4/k_{-4}$) in the context of Mechanism V, we assume that the [urea]-dependence of k_{-3} is wholly contained in k_{-3}^* for the following reason. The ratio of the calculated values of $\text{dln}k_3/\text{d[urea]}$ and $\text{dln}k_{-3}/\text{d[urea]}$ places roughly 70% of the overall [urea]-dependence of $\text{I}_2 \rightleftharpoons \text{RP}_o$ in k_3 ; this ratio is typical of the two-state folding of a globular protein, for which the forward rate constant (k_{fold}) generally contains $\sim 70\%$ of the overall [urea]-dependence, with the back rate constant (k_{unfold}) providing the remaining $\sim 30\%$.³¹ Since the forward elementary rate constant k_3 contains 70% of the overall [urea]-dependence, we surmise that the corresponding back direction elementary rate constant k_{-3}^* contains the remainder of the [urea]-dependence. The extension of this assumption is that the folding transition in RNAP implied by the [urea]-dependence is wholly contained within $\text{I}_2 \rightleftharpoons \text{I}_3$ ($K_3 = k_3/k_{-3}$).

Intermediate KCl concentrations

For the [KCl] upshift experiments, we find that equation (6) adequately models the dependence of $\text{ln}k_d$ on ln[KCl] throughout the range of KCl

concentrations studied. For the fits of the data to equation (6), shown as continuous lines in Figure 3(b), we used the values of k_{-2} and K_3^o in dissociation buffer at 37 °C and 10 °C determined from the fits of the [urea] upshift data (Table 3). As detailed in Methods, the best fits to the data necessitated the inclusion of a small temperature dependence of the equilibrium constant for the interaction of Mg^{2+} with the DNA phosphate backbone.

Fits of the [KCl] upshift data (Figure 3(b)) to equation (5) (which includes the k_{-2}/k_{-3} term in the expression for k_d ; equation (1)) did not improve the quality of the fit (not shown), suggesting that the quantity k_{-2}/k_{-3} does not significantly contribute to k_d at any KCl concentration. Use of equation (6) is consistent with the fact that the large [salt]-dependence of $\text{I}_2 \rightleftharpoons \text{RP}_o$ ($K_3 = k_3/k_{-3}$) likely stems from the formation of a new interface between RNAP and DNA. In general, for the formation of a protein-DNA interface, the dissociation-direction rate constant (the breaking of the interface, concurrent with the re-association of salt cations with the DNA phosphate backbone) is expected to be much more salt dependent (by roughly sixfold³⁶) than the forward-direction rate constant (in our case making

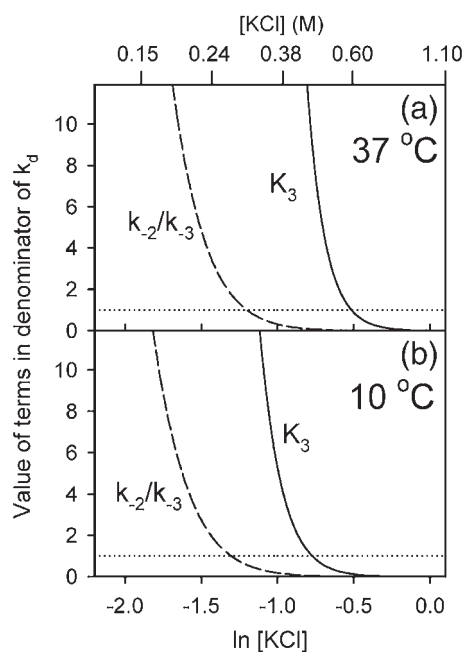


Figure 4. Predicted values of the terms in the denominator of the general expression for k_d ($=k_{-2}/(1+K_3+k_{-2}/k_{-3})$; equation (1)) as functions of ln [KCl] at 37 °C (a) and 10 °C (b). k_{-2}/k_{-3} is shown as a broken line, K_3 ($=k_3/k_{-3}$) is shown as a continuous line, and unity is shown as a horizontal dotted line. Values of K_3 were calculated throughout the range of [KCl] shown from the values of K_3^o in DB (Table 3) and equations (9)–(11). Values of k_{-3} used to calculate k_{-2}/k_{-3} were calculated from values of k_{-3}^o (Table 3) and equations (9)–(11) (with K_3 in the equations replaced by k_{-3}). The value of $S k_{-3}^{-\text{Mg}}$ used in equation (9) for calculating k_{-3} was 7.9 (assuming that $S k_{-3}$ is $\sim (6/7) S K_3$; see Analysis). Values of k_{-2} used to calculate k_{-2}/k_{-3} were calculated from the plateau values of k_d in Figure 3(b) (Table 3).

$Sk_{-3} \approx 6Sk_3$). Thus, k_{-2}/k_{-3} never becomes significant compared to K_3 , while K_3 still measurably contributes to k_d because $K_3 (=k_3/k_{-3})$ is much greater than k_{-2}/k_{-3} at low [KCl] and both terms decrease with similar [KCl]-dependences ($Sk_d \approx Sk_{-3}$). This is demonstrated in Figure 4, which shows the values of K_3 and k_{-2}/k_{-3} predicted by the parameters determined from our fits throughout the range of salt concentrations studied. In contrast to the [KCl] upshifts, the k_{-2}/k_{-3} term does become significant in our analysis of the [urea] upshifts because most of the [urea] dependence of K_3 is contained in k_3 (~70%). Thus, while K_3 is much larger than k_{-2}/k_{-3} at low [urea], and though both quantities decrease with increasing [urea], the [urea]-dependence of K_3 is much larger than that of k_{-2}/k_{-3} , and the two terms become comparable at an intermediate urea concentration (Figure 5).

Although it is likely that the [salt]-dependence of the composite rate constant for $RP_o \rightarrow I_2$ is much larger than that for $I_2 \rightarrow RP_o$, the individual contributions of $I_2 \rightleftharpoons I_3$ and $I_3 \rightleftharpoons RP_o$ in Mechanism V to the overall [salt]-dependence of $I_2 \rightleftharpoons RP_o$ cannot be determined from our data. Since the [salt]-dependence of k_d is assumed to result from the formation of a new RNAP-DNA interface, which is, in turn, likely coupled to the folding of a region of RNAP implied by the [urea]-dependence, we would expect most, if not all, of the [salt]-dependence of k_d to reside in the conversion of I_3 to I_2 .

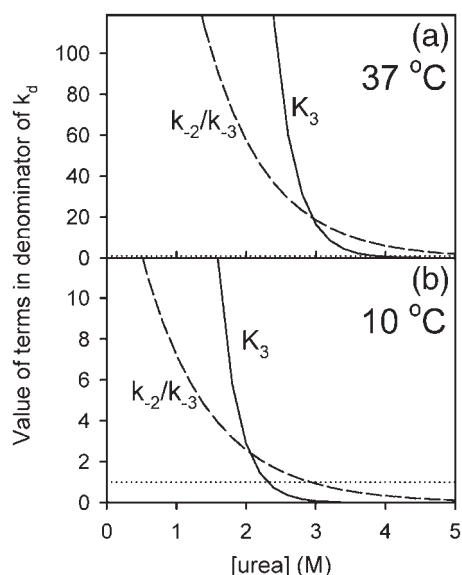


Figure 5. Values of the terms in the denominator of the general expression for $k_d (=k_{-2}/(1+K_3+k_{-2}/k_{-3})$; equation (1)) as functions of [urea] at 37 °C (a) and 10 °C (b). k_{-2}/k_{-3} is shown as a broken line, $K_3 (=k_3/k_{-3})$ is shown as a continuous line, and unity is shown as a horizontal dotted line. Values of K_3 were calculated throughout the range of [urea] shown from the values of K_3^o and $d\ln K_3/d[\text{urea}]$ (Table 3) and equation (7). Values of k_{-3} used to calculate k_{-2}/k_{-3} were calculated from values of k_{-3}^o and $d\ln k_{-3}/d[\text{urea}]$ (Table 3) and equation (8). Values of k_{-2} used to calculate k_{-2}/k_{-3} were calculated from the plateau values of k_d in Figure 3(a) (Table 3).

Discussion

The large [urea] and [salt]-dependences of $I_2 \rightleftharpoons RP_o$ are consistent with a large-scale folding transition and formation of a new RNAP-DNA interface

We previously interpreted the large increase in the rate of dissociation of RNAP- λP_R open complexes with increasing [urea] as reflecting the large-scale burial of polar amide surface (corresponding to the folding of ~120 amino acid residues) in the conversion of the transition state (I_1-I_2)[‡] into RP_o .¹¹ We proposed that the major folding process in which this surface is buried is the transition of disordered regions in the C terminus of the β' subunit, including parts of the downstream jaw of RNAP, to an ordered state, and that this transition occurs in $I_2 \rightleftharpoons RP_o$ (K_3 in Mechanism I).¹¹ (Over 100 conserved residues in this region of the C terminus of β' are predicted to be intrinsically disordered in free RNAP by the computer algorithm PONDR (predictor of naturally disordered regions^{37,38}.) The present study corroborates this large [urea] effect and provides strong evidence (see Analysis) that the folding transition does in fact occur in the conversion of I_2 to RP_o . Our deduction that the equilibrium constant K_3 for $I_2 \rightleftharpoons RP_o$ is also strongly [salt] dependent implies that a new RNAP-DNA interface is formed in the step. Located at the downstream end of the active site channel, the downstream jaw appears ideally positioned to fold onto the downstream DNA in RP_o formation, an interaction that could be the origin of the large [salt]-dependence of K_3 .

The lack of significant [urea] and [salt] effects on $I_1 \rightleftharpoons I_2$ indicate no change in the exposure of polar amide surface to the solvent and no net release/uptake of salt ions in this bottleneck step

We previously reported that the rate constant k_2 for $I_1 \rightarrow I_2$ is independent of urea concentration.¹¹ Based on the analysis of our current results described above, we deduce that the rate constant k_{-2} for $I_2 \rightarrow I_1$ and thus the equilibrium constant $K_2 (=k_2/k_{-2})$ for $I_1 \rightleftharpoons I_2$ are also independent of urea concentration. The lack of a measurable effect of [urea] on K_2 suggests that there is no significant net change in the amount of polar amide biopolymer surface exposed to the solvent, such as would result from a folding/unfolding transition in a region of RNAP, in $I_1 \rightleftharpoons I_2$. We also deduce that k_{-2} is independent of salt concentration. In a separate study, we find that k_2 is only slightly affected by salt concentration ($d\ln k_2/d\ln[\text{KCl}] = S k_2 \sim -1$ in the absence of Mg^{2+}) (Kontur *et al.* unpublished results). Thus, K_2 has only a slight dependence on salt concentration ($SK_2 \sim -1$), revealing that no significant net uptake or release of ions occurs in $I_1 \rightleftharpoons I_2$, such as would result from the burial/exposure of DNA phosphates and cationic groups on RNAP in

the formation/disruption of an RNAP-DNA interface. The lack of significant [urea] or [salt] effects on K_2 is surprising, as the interconversion of I_1 and I_2 is the rate-limiting bottleneck step in both the formation and dissociation of open complexes and would therefore be expected to involve large-scale conformational changes in RNAP and/or DNA. These findings lead us to propose that the major conformational change in $I_1 \rightleftharpoons I_2$ may occur within the active site channel of RNAP, largely shielded from the solution (and thus solute-inaccessible). This proposal is consistent with DNA backbone footprinting experiments,^{3,17} which reveal that both strands of the DNA are protected from cleavage from the -10 hexamer to ~+20 in both I_1 and RP_o .

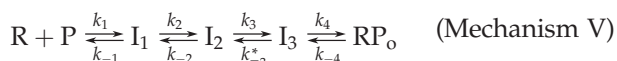
Defining conditions to structurally characterize the intermediate I_2

A major result of this study is the discovery that the open complex RP_o at the λP_R promoter can be shifted back to the uncharacterized, transient intermediate I_2 by a rapid upshift in urea or KCl concentration. In this burst experiment, a near-homogeneous population of I_2 is formed within the mixing time of a few milliseconds by an upshift to 1.1 M KCl or ~4 M urea, slowly decaying to I_1 on a time scale of approximately 1 s. This method provides a window of approximately 2 to 3 orders of magnitude in the time domain for structural characterization of I_2 by footprinting, cross-linking, or other chemical methods. Brenowitz and coworkers have recently developed a fast hydroxyl radical footprinting method that provides millisecond time scale capability to probe the DNA backbone.³⁹ Similarly, we observe that the permanganate footprinting of open DNA bases can be performed on a millisecond time scale using high concentrations of sodium permanganate (Kontur *et al.*, unpublished results). These fast reaction methods combined with rapid mixing will allow characterization of open bases and backbone protection in I_2 as compared to RP_o ^{3-5,40} and I_1 , the more stable intermediate recently characterized on the time course of open complex formation using manual mixing methods.¹⁷ Burst experiments with urea or salt provide the necessary large destabilization of RP_o relative to I_2 , which could not be achieved with downshifts to low temperature (see Results). Shifts of RP_o complexes at the λP_R promoter to low temperature^{3,35} now are understood to have destabilized RP_o with respect to I_1 but not with respect to I_2 , and therefore did not create a significant burst of I_2 .

Evidence for an additional step in the mechanism of open complex formation

As detailed in Analysis (and demonstrated in Figure 3(a)), the dependence of k_d on [urea] between ~1.5 M and 3.5 M urea at 10 °C and above ~2.5 M urea at 37 °C provides evidence for the possible existence of an additional kinetically-significant

intermediate (I_3) late in the mechanism of open complex formation:



We are currently testing Mechanism V with RNAP and DNA variants and with MnO_4^- footprinting experiments following upshift to high concentrations of KCl.

Materials and Methods

Buffers

Storage buffer for RNAP holoenzyme contained 50% (v/v) glycerol, 10 mM Tris-HCl (pH 7.5 at 4 °C), 100 mM NaCl, 0.1 mM DTT, and 0.1 mM Na_2EDTA . Dissociation buffer (DB) contained 10 mM (10.7 mM (millimolar)) $MgCl_2$, 41 mM (44 mM) Tris-HCl buffer (pH 8.0 at temperature of experiment), 884 mM (948 mM) glycerol, 1 mM (1 mM) DTT, 100 $\mu g/ml$ of bovine serum albumin (BSA), 13 mM (13.9 mM) NaCl, at least 120 mM (129 mM) KCl, and the final desired dissociation concentration of urea or additional KCl. In [urea] upshift experiments, concentrations of all species were held constant on the molal scale. In [KCl] upshift experiments, concentrations of all species were held constant on the molar scale. Wash buffer contained 0.1 M NaCl, 10 mM Tris-HCl (pH 8.0 at room temperature), and 0.1 mM Na_2EDTA .

Wild-type $E\sigma^{70}$ RNA polymerase holoenzyme

E. coli K12 wild-type RNA polymerase holoenzyme was purified as described⁴¹ and stored in storage buffer in 500 μl samples at -70 °C. All RNAP concentrations reported here refer to active concentrations, determined as described.⁶ Individual samples of RNAP used were 45-60% active.

λP_R promoter DNA

A DNA fragment containing the λP_R promoter was obtained from the plasmid pBR81 and labeled at the 3' end with ^{32}P as described.⁴⁰ The resulting blunt-ended fragment contains the λP_R wild-type sequence (from positions -60 to +20, relative to the transcription start site) centrally located in a DNA fragment extending from position -115 to +76. The specific activity of the fragment was generally ~ 10^{17} cpm/mol.

[Solute] upshift-induced dissociation kinetics

The irreversible kinetics of dissociation of RNAP-promoter DNA open complexes were measured at 10 °C and 37 °C using either manual mixing or rapid mixing, and nitrocellulose filter binding. Dissociation was initiated by addition of either urea or additional KCl, and the polyanionic competitor heparin.

i Manual mixing experiments

RNAP (final concentration 6-15 nM) and DNA (final concentration 0.05-0.5 nM) were combined in DB and

allowed to associate to equilibrium or completion either at the temperature at which dissociation was to occur or at room temperature. The pre-formed open complexes were incubated at the temperature of dissociation for at least 20 min before dissociation was initiated. (Longer times of incubation had no effect on the kinetics of the process.) At time $t=0$, the reaction was combined (in ≤ 10 s) with an equal volume of DB containing heparin and sufficient urea or additional KCl to obtain the final concentration of perturbant for the dissociation reaction (and 100 $\mu\text{g}/\text{ml}$ of heparin) for a final volume of 1–1.2 ml. At given time points, 100 μl of the reaction was filtered through nitrocellulose.

ii Rapid quench mixing experiments

RNAP (final concentration 5–30 nM) and DNA (final concentration 0.05–0.5 nM) were combined in DB and allowed to associate to completion at room temperature (30–60 min). Samples of these pre-formed open complexes in DB and of DB containing heparin (final concentration 100 $\mu\text{g}/\text{ml}$) and either urea or additional KCl were loaded into sample ports of a rapid mixer (Chemical-Quench-Flow model RQF-3; KinTek Co., Austin, TX) where they were incubated at the final temperature of dissociation for at least 5 min. A water bath was used to regulate the temperature of the reaction loops in the apparatus (monitored by a Fluke 51K/J temperature probe). At time zero, known (approximately equal) volumes of the two samples were rapidly mixed (in less than 20 ms) in the reaction loop, resulting in final concentrations of 100 $\mu\text{g}/\text{ml}$ of heparin and the reported dissociation concentrations of urea or KCl. The solutions used to push the two reactant solutions together matched the reactant solutions in composition. At time t , the reaction was rapidly combined with “quench solution” (a buffered low [KCl] solution), effectively stopping the dissociation reaction by diluting perturbant concentrations to 0.08–0.12 M KCl and <1.5 M urea at room temperature. The quenched sample was collected and filtered through nitrocellulose at room temperature.

Nitrocellulose filter binding assays

Nitrocellulose filter binding assays were performed as described.¹¹ As nitrocellulose retains RNAP but not dsDNA, the only radioactive DNA remaining on the nitrocellulose after filtering and rinsing with wash buffer is that still complexed with RNAP. For manual mixing reactions, the total counts per minute filtered (cpm_{TOT} , generally ~ 1000 – 3500 cpm) was determined by spotting 20 μl from the reaction mixture onto a dried nitrocellulose filter. For rapid mixing reactions, cpm_{TOT} was determined by performing a reaction and applying the entire expelled sample to three dried nitrocellulose filters. Background retention of radiolabeled DNA on filters (cpm_{bkgd}) was determined by filtering an aliquot of the reaction mixture lacking RNAP. Filter efficiency (FE; the fraction of label retained on a filter under conditions where all promoter DNA in solution is complexed as open complexes) for a given perturbant concentration was determined by dividing the extrapolated intercept from a reaction performed at 37 °C by cpm_{TOT} from the reaction. Filter efficiencies were generally ~ 0.70 – 0.95 , and were not found to be significantly affected by perturbant up to 0.24 M KCl and 1.5 M urea. (All higher concentrations of perturbant were diluted to lower perturbant concentrations before filtering). The observed fraction of promoter DNA in the form of open complexes at a given time

point (θ_{obs}) was determined by dividing the counts per minute ($\text{cpm}_t = \text{cpm}_{\text{obs}} - \text{cpm}_{\text{bkgd}}$) by the total counts per minute, cpm_{TOT} . θ_{obs} was corrected for filter efficiency to determine the fraction of promoter DNA capable of binding to RNAP in the form of open complexes, $\theta_t \left(= \frac{1}{\text{FE}} \theta_{\text{obs}} \right)$.

Data analysis

Fitting of dissociation data to single-exponential decay

The observed rate constant (k_d) for the irreversible dissociation of open complexes was determined by fitting θ_t versus time for a given perturbant concentration to a single-exponential decay equation:

$$\theta_t = \theta_t^0 e^{-k_d t} \quad (4)$$

where θ_t^0 is the value of θ_t at time $t=0$.

Dependences of $\ln k_d$ on [urea] and on \ln [KCl]

Expressions for the dependence of $\ln k_d$ on [perturbant] are as follow (depending on whether k_{-2}/k_{-3} is significant compared to K_3 ; see Eqs. 1 and 2):

$$\ln k_d = \ln k_{-2} - \ln \left(1 + K_3 + \frac{k_{-2}}{k_{-3}} \right) \quad (5)$$

(based on equation (1))

$$\ln k_d = \ln k_{-2} - \ln(1 + K_3) \quad (6)$$

(based on equation (2a))

where both K_3 and k_{-3} are functions of KCl and urea concentration.

The expressions for K_3 and k_{-3} as functions of [urea] in equations (5) and (6) are (assuming that $\ln K_3$ and $\ln k_{-3}$ are both linearly dependent on [urea]):

$$K_3 = K_3^0 \exp \left(\frac{d \ln K_3}{d [\text{urea}]} [\text{urea}] \right) \quad (7)$$

$$k_{-3} = k_{-3}^0 \exp \left(\frac{d \ln k_{-3}}{d [\text{urea}]} [\text{urea}] \right) \quad (8)$$

where K_3^0 and k_{-3}^0 are the values of K_3 and k_{-3} in DB in the absence of urea. Data as a function of [urea] at 37 °C and 10 °C were globally fit together. To minimize the number of parameters, the dependence of k_{-3} on [urea] was assumed to be temperature-independent.

K_3 was determined as a function of [KCl] according to:

$$\ln K_3 = \ln K_3^0 - S K_3^{-M_g} \ln([KCl]/0.120) - \left(\frac{S K_3^{-M_g}}{0.88} \right) \ln \left(S^{120 \text{ mM}} / S^{[KCl]} \right) \quad (9)$$

where: K_3^0 is the value of K_3 in DB; SK_3^{-Mg} is the value of SK_3 in the absence of Mg^{2+} ($SK_3^{-Mg} = -9.2$ (W. S.K. *et al.*, unpublished results)):

$$S^{[KCl]} = 0.5(1 + (1 + 4 K_{obs}^{Mg} [Mg^{2+}])^{0.5})$$

at the KCl concentration being considered

(10)

K_{obs}^{Mg} is the equilibrium constant for the association of Mg^{2+} with the DNA phosphate backbone. The best fits of the data at 10 °C and 37 °C necessitated using different expressions for K_{obs}^{Mg} as a function of [KCl], implying a temperature dependence of K_{obs}^{Mg} at a given KCl concentration:

$$\log K_{obs}^{Mg} = -1.3 \log[KCl] + 0.40 \quad (37 \text{ }^\circ\text{C}) \quad (11a)$$

$$\log K_{obs}^{Mg} = -1.6 \log[KCl] + 0.60 \quad (10 \text{ }^\circ\text{C}) \quad (11b)$$

Acknowledgements

This research was supported by NIH grant GM23467. W.S.K. acknowledges support from NIH 5 T32 GM08349. The authors thank Oleg Tsodikov for helpful early discussions regarding analysis of the data. We thank the reviewer and editor for their careful reading of the manuscript and helpful suggestions.

References

- Lin, Y. C., Choi, W. S. & Gralla, J. D. (2005). TFIIF XBP mutants suggest a unified bacterial-like mechanism for promoter opening but not escape. *Nature Struct. Mol. Biol.* **12**, 603–607.
- Darst, S. A. (2001). Bacterial RNA polymerase. *Curr. Opin. Struct. Biol.* **11**, 155–162.
- Craig, M. L., Tsodikov, O. V., McQuade, K. L., Schlax, P. E., Jr, Capp, M. W., Saecker, R. M. & Record, M. T., Jr (1998). DNA footprints of the two kinetically significant intermediates in formation of an RNA polymerase-promoter open complex: evidence that interactions with start site and downstream DNA induce sequential conformational changes in polymerase and DNA. *J. Mol. Biol.* **283**, 741–756.
- Raffaella M. (2003). Characterization by DNA footprinting of intermediates involved in transcription initiation by *Escherichia coli* $E\sigma^{70}$ RNA polymerase at the λP_R promoter. PhD thesis, University of Wisconsin-Madison.
- Suh, W. C., Ross, W. & Record, M. T., Jr (1993). Two open complexes and a requirement for Mg^{2+} to open the λP_R transcription start site. *Science*, **259**, 358–361.
- Roe, J. H., Burgess, R. R. & Record, M. T., Jr (1984). Kinetics and mechanism of the interaction of *Escherichia coli* RNA polymerase with the λP_R promoter. *J. Mol. Biol.* **176**, 495–522.
- Roe, J. H. & Record, M. T., Jr (1985). Regulation of the kinetics of the interaction of *Escherichia coli* RNA polymerase with the λP_R promoter by salt concentration. *Biochemistry*, **24**, 4721–4726.
- Roe, J. H., Burgess, R. R. & Record, M. T., Jr (1985). Temperature dependence of the rate constants of the *Escherichia coli* RNA polymerase- λP_R promoter interaction. Assignment of the kinetic steps corresponding to protein conformational change and DNA opening. *J. Mol. Biol.* **184**, 441–453.
- Saecker, R. M., Tsodikov, O. V., McQuade, K. L., Schlax, P. E., Jr, Capp, M. W. & Record, M. T., Jr (2002). Kinetic studies and structural models of the association of *E. coli* σ^{70} RNA polymerase with the λP_R promoter: large scale conformational changes in forming the kinetically significant intermediates. *J. Mol. Biol.* **319**, 649–671.
- Tsodikov, O. V. & Record, M. T., Jr (1999). General method of analysis of kinetic equations for multistep reversible mechanisms in the single-exponential regime: application to kinetics of open complex formation between $E\sigma^{70}$ RNA polymerase and lambdaP(R) promoter DNA. *Biophys. J.* **76**, 1320–1329.
- Kontur, W. S., Saecker, R. M., Davis, C. A., Capp, M. W. & Record, M. T. (2006). Solute probes of conformational changes in open complex RP_o formation by *Escherichia coli* RNA polymerase at the λP_R promoter: evidence for unmasking of the active site in the isomerization step and for large-scale coupled folding in the subsequent conversion to RP_o . *Biochemistry*, **45**, 2161–2177.
- Suh, W. C., Leirimo, S. & Record, M. T. (1992). Roles of Mg^{2+} in the mechanism of formation and dissociation of open complexes between *Escherichia coli* RNA polymerase and the λP_R promoter: kinetic evidence for a second open complex requiring Mg^{2+} . *Biochemistry*, **31**, 7815–7825.
- McQuade, K. L. (1996). $E\sigma^{70}$ RNA polymerase- λP_R promoter interactions: effects of temperature and initiating nucleotides on the kinetics and thermodynamics of open complex formation. PhD thesis, University of Wisconsin-Madison.
- Spolar, R. S. & Record, M. T., Jr (1994). Coupling of local folding to site-specific binding of proteins to DNA. *Science*, **263**, 777–784.
- Paul, B. J., Barker, M. M., Ross, W., Schneider, D. A., Webb, C., Foster, J. W. & Gourse, R. L. (2004). DksA: a critical component of the transcription initiation machinery that potentiates the regulation of rRNA promoters by ppGpp and the initiating NTP. *Cell*, **118**, 311–322.
- Paul, B. J., Berkmen, M. B. & Gourse, R. L. (2005). DksA potentiates direct activation of amino acid promoters by ppGpp. *Proc. Natl. Acad. Sci. USA*, **102**, 7823–7828.
- Davis, C. A., Bingman, C. A., Landick, R., Record, M. T., Jr & Saecker, R. M. (2007). Real-time footprinting of DNA in the first kinetically significant intermediate in open complex formation by *Escherichia coli* RNA polymerase. *Proc. Natl. Acad. Sci. U S A*, **104**, 7833–7838.
- Spassky, A., Kirkegaard, K. & Buc, H. (1985). Changes in the DNA structure of the lac UV5 promoter during formation of an open complex with *Escherichia coli* RNA polymerase. *Biochemistry*, **24**, 2723–2731.
- Buc, H. & McClure, W. R. (1985). Kinetics of open complex formation between *Escherichia coli* RNA polymerase and the lac UV5 promoter. Evidence for a sequential mechanism involving three steps. *Biochemistry*, **24**, 2712–2723.
- McKane, M. & Gussin, G. N. (2000). Changes in the 17 bp spacer in the λP_R promoter of bacteriophage lambda affect steps in open complex formation that

- precede DNA strand separation. *J. Mol. Biol.* **299**, 337–349.
21. Brodolin, K. & Buckle, M. (2001). Differential melting of the transcription start site associated with changes in RNA polymerase-promoter contacts in initiating transcription complexes. *J. Mol. Biol.* **307**, 25–30.
 22. Buckle, M., Pemberton, I. K., Jacquet, M. A. & Buc, H. (1999). The kinetics of sigma subunit directed promoter recognition by *E. coli* RNA polymerase. *J. Mol. Biol.* **285**, 955–964.
 23. Auton, M., Holthausen, L. M. & Bolen, D. W. (2007). Anatomy of energetic changes accompanying urea-induced protein denaturation. *Proc. Natl. Acad. Sci. USA*, **104**, 15317–15322.
 24. Cannon, J. G., Anderson, C. F. & Record, M. T., Jr (2007). Urea-amide preferential interactions in water: quantitative comparison of model compound data with biopolymer results using water accessible surface areas. *J. Phys. Chem. ser. B*, **111**, 9675–9685.
 25. Hong, J., Capp, M. W., Anderson, C. F., Saecker, R. M., Felitsky, D. J., Anderson, M. W. & Record, M. T., Jr (2004). Preferential interactions of glycine betaine and of urea with DNA: implications for DNA hydration and for effects of these solutes on DNA stability. *Biochemistry*, **43**, 14744–14758.
 26. Scholtz, J. M., Barrick, D., York, E. J., Stewart, J. M. & Baldwin, R. L. (1995). Urea unfolding of peptide helices as a model for interpreting protein unfolding. *Proc. Natl. Acad. Sci. USA*, **92**, 185–189.
 27. Courtenay, E. S., Capp, M. W., Saecker, R. M. & Record, M. T., Jr (2000). Thermodynamic analysis of interactions between denaturants and protein surface exposed on unfolding: interpretation of urea and guanidinium chloride m-values and their correlation with changes in accessible surface area (ASA) using preferential interaction coefficients and the local-bulk domain model. *Proteins: Struct. Funct. Genet.* **4**, 72–85.
 28. Courtenay, E. S., Capp, M. W. & Record, M. T., Jr (2001). Thermodynamics of interactions of urea and guanidinium salts with protein surface: relationship between solute effects on protein processes and changes in water-accessible surface area. *Protein Sci.* **10**, 2485–2497.
 29. Felitsky, D. J. & Record, M. T., Jr (2003). Thermal and urea-induced unfolding of the marginally stable lac repressor DNA-binding domain: a model system for analysis of solute effects on protein processes. *Biochemistry*, **42**, 2202–2217.
 30. Hong, J., Capp, M. W., Saecker, R. M. & Record, M. T., Jr (2005). Use of urea and glycine betaine to quantify coupled folding and probe the burial of DNA phosphates in lac repressor-lac operator binding. *Biochemistry*, **44**, 16896–16911.
 31. Plaxco, K. W., Simons, K. T. & Baker, D. (1998). Contact order, transition state placement and the refolding rates of single domain proteins. *J. Mol. Biol.* **277**, 985–994.
 32. Berg, D. & Chamberlin, M. (1970). Physical studies on ribonucleic acid polymerase from *Escherichia coli* B. *Biochemistry*, **9**, 5055–5064.
 33. Inman, R. B. & Baldwin, R. L. (1962). Helix-random coil transitions in synthetic DNAs of alternating sequence. *J. Mol. Biol.* **5**, 172–184.
 34. Record, M. T., Jr, Anderson, C. F. & Lohman, T. M. (1978). Thermodynamic analysis of ion effects on the binding and conformational equilibria of proteins and nucleic acids: the roles of ion association or release, screening, and ion effects on water activity. *Quart. Rev. Biophys.* **11**, 103–178.
 35. Tsodikov, O. V., Craig, M. L., Saecker, R. M. & Record, M. T., Jr (1998). Quantitative analysis of multiple-hit footprinting studies to characterize DNA conformational changes in protein-DNA complexes: application to DNA opening by $E\sigma^{70}$ RNA polymerase. *J. Mol. Biol.* **283**, 757–769.
 36. Lohman, T. M., DeHaseth, P. L. & Record, M. T., Jr (1978). Analysis of ion concentration effects of the kinetics of protein-nucleic acid interactions. Application to lac repressor-operator interactions. *Biophys. Chem.* **8**, 281–294.
 37. Romero, P., Obradovic, Z., Li, X., Garner, E. C., Brown, C. J. & Dunker, A. K. (2001). Sequence complexity of disordered protein. *Proteins: Struct. Funct. Genet.* **42**, 38–48.
 38. Li, X., Romero, P., Rani, M., Dunker, A. K. & Obradovic, Z. (1999). Predicting protein disorder for N-, C-, and internal regions. *Genome Inform. Ser. Workshop Genome Inform.* **10**, 30–40.
 39. Shcherbakova, I., Mitra, S., Beer, R. H. & Brenowitz, M. (2006). Fast Fenton footprinting: a laboratory-based method for the time-resolved analysis of DNA, RNA and proteins. *Nucl. Acids. Res.* **34**, e48; Published online 2006 March 31.
 40. Craig, M. L., Suh, W. C. & Record, M. T., Jr (1995). HO^{\bullet} and DNase I probing of $E\sigma^{70}$ RNA polymerase- λP_R promoter open complexes: Mg^{2+} binding and its structural consequences at the transcription start site. *Biochemistry*, **34**, 15624–15632.
 41. Burgess, R. R. & Jendrisak, J. J. (1975). A procedure for the rapid, large-scale purification of *Escherichia coli* DNA-dependent RNA polymerase involving Polymin P precipitation and DNA-cellulose chromatography. *Biochemistry*, **14**, 4634–4638.